

A self-supervised CNN for image watermark removal

Chunwei Tian, *Member, IEEE*, Menghua Zheng, Tiancai Jiao, Wangmeng Zuo, *Senior Member, IEEE*, Yanning Zhang, *Senior Member, IEEE*, Chia-Wen Lin, *Fellow, IEEE*

Abstract—Popular convolutional neural networks mainly use paired images in a supervised way for image watermark removal. However, watermarked images do not have reference images in the real world, which results in poor robustness of image watermark removal techniques. In this paper, we propose a self-supervised convolutional neural network (CNN) in image watermark removal (SWCNN). SWCNN uses a self-supervised way to construct reference watermarked images rather than given paired training samples, according to watermark distribution. A heterogeneous U-Net architecture is used to extract more complementary structural information via simple components for image watermark removal. Taking into account texture information, a mixed loss is exploited to improve visual effects of image watermark removal. Besides, a watermark dataset is conducted. Experimental results show that the proposed SWCNN is superior to popular CNNs in image watermark removal. Codes can be obtained at <https://github.com/helloxiaotian/SWCNN>.

Index Terms—Self-supervised learning, CNN, perception theory, image watermark removal.

I. INTRODUCTION

Due to developments of big data and internet techniques, images have become a medium of office and entertainment. To protect copyrights of these images, watermarks (i.e., letter, number and logos) are conducted on given images to protect material [1, 2]. Although these watermarks can claim ownerships of protected images under certain conditions, they are faced with some challenges of robustness of watermark

This work was supported in part by the National Natural Science Foundation of China under Grant 62201468, in part by the China Postdoctoral Science Foundation under Grant 2022TQ0259 and 2022M722599.

(Corresponding author: Yanning Zhang (Email: ynzhang@nwpu.edu.cn), Chia-Wen Lin (Email: cwlin@ee.nthu.edu.tw))

Chunwei Tian is with the School of Software, Northwestern Polytechnical University, Xi'an, Shaanxi, 710129, China. Also, he is with the National Engineering Laboratory for Integrated Aero-Space-Ground-Ocean Big Data Application Technology, Xi'an, Shaanxi, 710129, China. (Email: chunweitian@nwpu.edu.cn)

Menghua Zheng is with the School of Software, Northwestern Polytechnical University, Xi'an, Shaanxi, 710129, China. (Email: menghuazheng@mail.nwpu.edu.cn)

Tiancai Jiao is with the School of Software, Northwestern Polytechnical University, Xi'an, Shaanxi, 710129, China. (Email: jtc@mail.edu.nwpu.cn)

Wangmeng Zuo is with the School of Computer Science and Technology, Harbin Institute of Technology, Harbin, Heilongjiang, 150001, China. Also, he is with the Peng Cheng Laboratory, Shenzhen, Guangdong, 518055, China. (Email: wzmzuo@hit.edu.cn)

Yanning Zhang is with the School of Computer Science, Northwestern Polytechnical University, the National Engineering Laboratory for Integrated Aero-Space-Ground-Ocean Big Data Application Technology, Xi'an, Shaanxi, 710129, China. (Email: ynzhang@nwpu.edu.cn)

Chia-Wen Lin is with the Department of Electrical Engineering and the Institute of Communications Engineering, National Tsing Hua University, Hsinchu300, Taiwan (E-mail: cwlin@ee.nthu.edu.tw)

techniques and network security [3]. To test quality of these watermarks, image watermark attack methods are presented [4].

Using multiple destruction, i.e., JPEG compression, low-pass filtering and noise pollution can attack watermarked images to verify robustness of a watermarking algorithm [5]. Alternatively, removing image watermarks is also a good choice to protect copyright of added watermarks and protected clean images [6]. For instance, exploiting correct user keys in the wavelet domain can effectively remove watermarks to obtain clean images to protect copyright of users [6]. Combining user key and hidden data in the non-watermarked area can help users to remove embedded watermarks to obtain clean images [7]. Additionally, the cross-channel correlation from color images and structural information are used to repair areas damaged by watermark [8]. Using locally dependent parts of given watermark images can automated remove watermarks [9]. Taking into efficiency account, combining Canny edge operator, Otsu thresholding and total variation can deal with structure and texture images for enhancing attack ability [10]. Although these methods have obtained good effects in image watermark removal, they may suffer from drawbacks of manual tuning parameters and complex optimization parameter methods.

To resolve these issues, deep networks with architectures of black boxes are presented in computer vision tasks [11, 12]. For instance, Tian et al. used heterogeneous convolutions to extract horizontal and vertical key features to enhance visual effects in image super-resolution tasks [13]. Due to strong learning ability, deep networks are also extended to image watermark removal [14]. A deep network with a fine-tuning operation can use fewer data to train a good image watermark removal model [15]. To test effectiveness of visible watermarks, a common framework based on a CNN is used to detect and remove watermarks [16]. To deal with watermark removal of realistic watermarked images, generative adversarial networks (GANs) are developed [17]. Fusing a GAN and self-attention mechanism can remove watermarks of unknown locations to obtain high-quality images [18]. Besides, using elastic weight consolidation and unlabeled data augmentation to implement a fine-tuning framework can effectively deal with image watermark removal [19]. To restore more texture details, a two-stage network containing a multi-task network and an attention is designed to recover more texture information rather than detecting watermark locations for watermark removal [20]. Due to a barrier of uncertainty, i.e., size, shape and color, a two-phase network is presented [21]. That is, the first

phase is used to obtain a rough decomposition via a given watermarked image. The second phase is exploited to remove watermark via centers on a watermark area. To extract robust watermark features, a cascaded U-Net network is conducted for watermark removal [22]. Although these methods have obtained excellent performance for verifying robustness of image watermark removal, most of these methods require ground truth to train image watermark removal models, which is limited by real digital camera devices.

In this paper, we present a self-supervised convolutional neural network for image watermark removal as well as SWCNN. SWCNN utilizes a self-supervised mechanism to obtain reference watermarked images to test quality of added watermarks. Also, a heterogeneous U-Net architecture uses simple components to extract more complementary structural information for image watermark removal. To further improve quality of predicted images, a mixed loss is exploited to counterpoise structural information and texture information. Besides, a watermark dataset is conducted. The proposed SWCNN has obtained excellent results to verify watermark quality.

Contributions of the proposed SWCNN can be summarized as follows.

(1) A self-supervised mechanism is proposed to construct reference watermarked images rather than giving paired watermarked images.

(2) A heterogeneous U-Net with simple components is designed to obtain more hierarchical and complementary structural information in image watermark removal.

(3) A mixed loss is utilized to extract more structural information and texture information for improving robustness of the proposed image watermark removal method.

(4) A watermark dataset is conducted via twelve novel watermarks, which is very convenient to engineers and scholars for commercial and civil.

Remaining parts of this paper can be summarized as follows. Section II gives proposed method. Section III illustrates experiments. Section IV describes conclusion.

II. PROPOSED METHOD

A. Self-supervised Mechanism

It is known that most of existing image watermark removal methods depend on paired watermarked image and non-watermarked image to verify their robustness [23]. However, real watermarked images do not have reference clean images, which limits their applications on real digital camera devices. That can be address by machine learning [24]. That is, we assume that we test temperature of a fixed room many times to obtain unreliable results, i.e., $y = y_1, y_2, \dots$. To obtain true temperature, a common method uses a discriminant function (also treated as loss function) D to obtain a smallest average deviation to find a number g [24], which can be formulated as Eq. (1).

$$\arg \min_g E_y \{D\{(g, y)\}, \quad (1)$$

When D is a L2 loss function and $D(g, y) = (g - y)^2$, its optimization solution can be obtained via $g = E_y(y)$.

When D is a L1 loss function and $D(g, y) = |g - y|$, its optimization solution can be obtained by the $g = \text{median}\{y\}$. According to a statistical idea, common estimation can convert a loss function as a negative log likelihood function [24]. Also, training of a neural network is suitable to mentioned principle. Its training procedure can be expressed as Eq. (2).

$$\arg \min_{\theta} E_{(i,o)} (D(f_{\theta}(i), o)), \quad (2)$$

where i and o are an input and a target, respectively. θ denotes parameters. Also, f stands for a network function.

According to Bayesian theory, Eq. (2) can be replaced with Eq. (3) [24].

$$\arg \min_{\theta} E_i \{E_{o|i} \{D\{f_{\theta}(i), o\}\}\} \quad (3)$$

It is known that input-conditioned target distributions can be transformed to arbitrary distributions when they have same conditional expected values. Thus, Eq. (3) can be further optimized as Eq. (4) [24].

$$\arg \min_{\theta} \sum_j D(f_{\theta}(i_j^1), o_j^1), \quad (4)$$

where predicted value and target have noisy distribution and they are suitable to $E\{o_j^1 | i_j^1\} = o_j$. Thus, different noisy images with same distribution noise can be conducted as paired noisy image dataset. Inspired by noise-to-noise idea [24], we propose a self-supervised mechanism to construct paired data of a watermarked image and reference image. That is, watermarks randomly added once on a given clean image is considered as a watermarked image and watermarks randomly added another is treated as a reference image to construct a paired of images between a watermarked image and reference image to conduct a training dataset where watermarked images are conducted via the mentioned illustrations. Also, watermarked images are conducted via the following equation [25].

$$I_w(pi) = \alpha(pi)W(pi) + (1 - \alpha(pi))I_c, \quad (5)$$

where $pi(x, y)$ is a pixel location. $\alpha(pi)$ denotes spatially varying opacity. I_w stands for a watermarked image and W is used to represent a watermark. I_c is utilized to symbol a natural image. More information can be found in Ref. [25].

B. Network Architecture of Self-supervised Convolutional Neural Network

The SWCNN contains three parts, i.e., a self-supervised mechanism (SSM), an 18-layer heterogeneous network (HN) and a perception network (PN). The SSM uses noise-to-noise [24] to construct reference watermarked images. The HN containing different activation functions, pooling functions, convolutional layers, concatenation operations and transpose convolutions uses obtained paired watermarked images and reference watermarked images from SSM to achieve heterogeneous U-Net architecture for facilitating more complementary structural information in image watermark removal. To obtain more texture information, a PN uses results of middle layers of trained a classifier by the ImageNet [26] as well as PN1 in Fig. 1 to detect quality of obtained texture information. To visually express the mentioned process of SWCNN, we define the following equation.

$$\begin{aligned} O_{SWCNN} &= f_{SWCNN}(I_w) \\ &= f_{PN1}(f_{HN}(I_w)), \end{aligned} \quad (6)$$

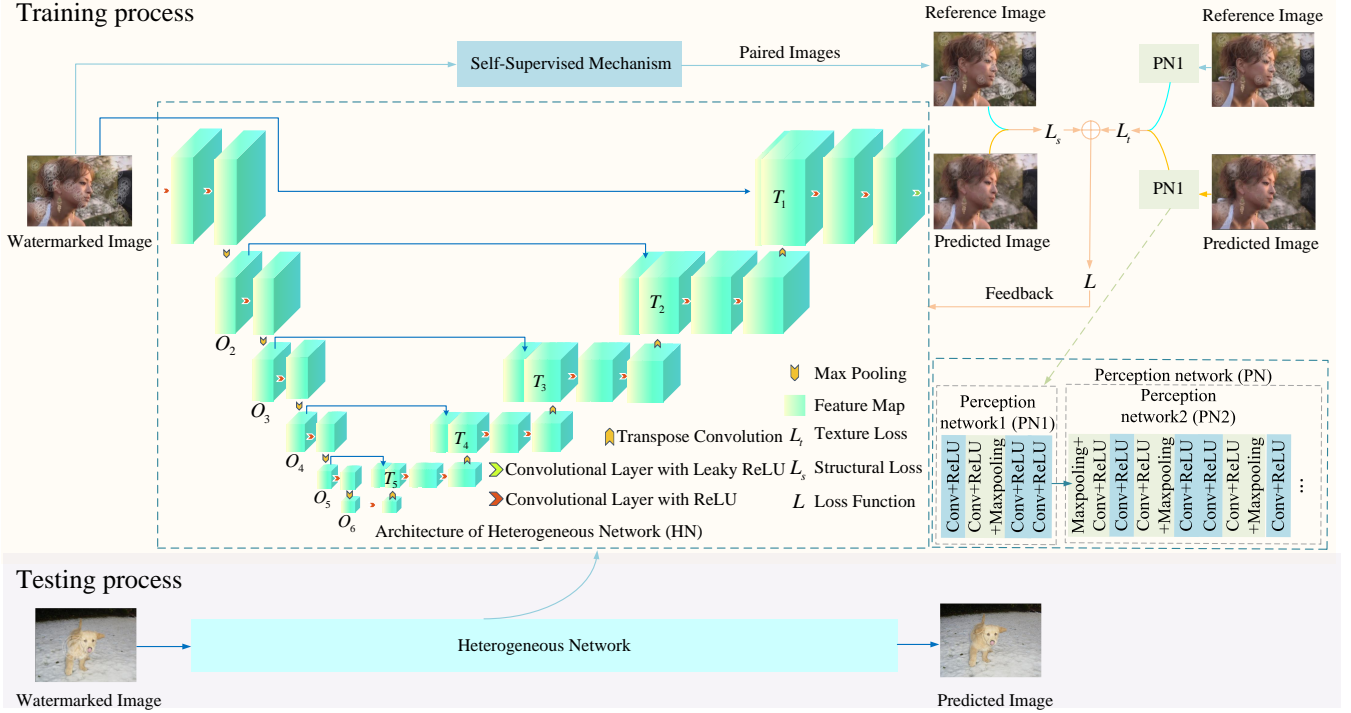


Fig. 1. Architecture of SWCNN.

where I_w denotes given watermarked images, f_{SWCNN} is function of SWCNN, f_{PN1} and f_{HN} represents functions of PN1 and HN. Also, O_{SWCNN} is utilized to express the output of SWCNN. f_{SWCNN} is obtained by the following loss function and training data from the SSM as shown Section II.E.

C. Heterogenous Network

18-layer heterogeneous network as well as HN [24] containing some components, i.e., convolutional layers, ReLU [26], Leaky ReLU [27], max pooling operations, concatenation operations and transpose convolutions is used to extract different features for improving facilitating more complementary structural information in image watermark. The 1st, 8th, 10th, 12th, 14th, 16th and 17th layers are composed of a combination of a convolutional layer and ReLU. The 2nd, 3rd, 4th, 5th and 6th layers consist of a combination of a convolutional layer, ReLU and max pooling. The 7th, 9th, 11th, 13th and 15th layers include a combination of a convolutional layer, ReLU and transpose convolution. The 18th layer contains a combination of a convolutional layer and Leaky ReLU. To improve memory ability of the HN, concatenation operations are acted on different layers. That is, given watermarked images and obtained information of the 15th layer are concatenated as input of the 16th layer in the HN. Obtained features of the 2nd and 13th layers are fused via a concatenation operation to act the 14th layer in the HN. Obtained information of the 3rd and 11th layers are integrated via a concatenation operation to act the 12th layer in the HN. Obtained information of the 4th and 9th layers are integrated via a concatenation operation to act the 10th layer in the HN. Obtained information of the 5th and 7th layers are integrated via a concatenation operation

to act the 8th layer in the HN. Kernel sizes of all the layers are 3×3 . The 1st layer has input channels of 3 and output channels of 48. Input and output channel number of the 2nd-7th layers are 48, respectively. The 8th and 9th layer have input channels of 96 and output channels of 96. The 10th, 12th and 14th layer have input channels of 144 and output channels of 96. The 11th, 13th and 15th layer have input channels of 96 and output channels of 96. The 16th layer has input channels of 99 and output channels of 64. The 17th layer has input channels of 64 and output channels of 32. The 18th layer has input channels of 32 and 3. The mentioned illustrations can be formulated as follows.

$$O_{HN} = f_{HN}(I_w) = CLR(CR(CR(Cat(I_w, T_1)))) \quad (7)$$

$$T_i = CRTC(CR(Cat(O_{i+1}, T_{i+1}))) (i = 1, 2, 3, 4) \quad (8)$$

$$T_5 = CRTC(O_6) \quad (9)$$

$$O_2 = CRMP(CR(I_w)), \quad (10)$$

$$O_3 = 2CRMP(CR(I_w)), \quad (11)$$

$$O_4 = 3CRMP(CR(I_w)), \quad (12)$$

$$O_5 = 4CRMP(CR(I_w)), \quad (13)$$

$$O_6 = 5CRMP(CR(I_w)), \quad (14)$$

where Cat is a concatenation operation, $CRTC$ is defined as a combination of CR (also regarded as a combination of a convolutional layer and a ReLU), Transpose convolution. CLR is the combination of a convolutional layer and a Leaky ReLU. $CRMP$ is utilized to represent a convolutional layer, a ReLU and a Maxpooling operation. O_i expresses an output of the i th layer in the heterogeneous network, where $i=2,3,4,5,6$. T_i expresses an output of the i th transpose convolutional layer in the heterogeneous network, where $i=1,2,3,4,5$. $iCRMP$

denotes i stacked CRMP, where $i = 2, 3, 4, 5$. And O_{HN} stands for a predicted image of the heterogeneous network.

D. Perception Network

Perception network is implemented via a VGG architecture [17]. That is, we use VGG on ImageNet to train a classifier. Subsequently, we put predicted results of HN and obtained reference image as inputs of PN (The first four layers of PN are composed of PN1), respectively. The outputs of 4th layer in the PN from mentioned different inputs are used to compute loss value of a texture loss. f_{PN1} in Eq. (6) can be represented as Eq. (15).

$$f_{PN1} = CR(CR(CRMP(CR(f_{vgg}))))), \quad (15)$$

where f_{vgg} is denoted as a function of VGG, which can be shown in Ref. [17]. Also, network architecture of PN1 can be visually shown in Fig.1.

E. Loss Function

Taking into structural and texture information account, we propose a mixed loss based L1, which contains two parts, i.e., a structural loss and texture loss. The structural loss function is responsible for monitoring robustness of extracting structural features from a heterogeneous network. Also, the texture loss is used to monitor robustness of obtaining texture information from a perception network, where texture information is intermediate results of a classification network via the ImageNet. To improve training speed, mentioned loss functions are implemented by L1. Besides, training data is obtained by a self-supervised mechanism in Section II.C. To vividly express mentioned mixed loss, the following equation is conducted.

$$\begin{aligned} L &= L_s + \lambda L_t \\ &= 1/N \sum_{i=1}^N |f_{HN}(I_w^i) - I_r^i| + \lambda |f_{PN1}(f_{HN}(I_w^i)) - f_{PN1}(I_r^i)|, \end{aligned} \quad (16)$$

where L , L_t and L_s are used to denote loss functions of the SWCNN, structural loss function and texture information, respectively. λ is the adjustment coefficient for the texture information. N is the number of watermarked images. I_r^i is used to represent the i th obtained reference image and I_w^i is exploited to the i th watermarked image, which can be introduced in Section II.A. Besides, the trained model relies on Adam [28] to optimize parameters.

According to mentioned illustrations, we can see that the proposed mixed loss is composed of two parts, i.e., a structural loss and texture loss. The structural loss depends on HN, which is conducted as follows.

$$\begin{aligned} L_s &= 1/N \sum_{i=1}^N |f_{HN}(I_w^i) - I_r^i| \\ &= 1/N \sum_{i=1}^N |O_{HN}^i - I_r^i|, \end{aligned} \quad (17)$$

where O_{HN}^i is the HN output of the i th image. The texture loss relies on PN, which can be shown in Section II. D.

III. EXPERIMENTS

A. Conducted datasets

To make obtained watermark method more robust, we collect a training and test datasets based an image with more watermarks rather than an image with one watermark.

Training datasets: We choose 477 representative natural images with format of ‘.jpg’ from the PASCAL VOC 2012 [29]. Specifically, each watermarked image of training dataset randomly uses one of twelve watermarks in Fig. 2 with one transparency from 0.3, 0.5, 0.7 and 1.0, from 0 to 0.4 in coverage in a self-supervised way in Section II.A is conducted, where watermark size is set 0.5-1 times. To accelerate training speed, each watermark image is cropped as 3,111 patches with 256×256 .

Test datasets: We choose 27 representative natural images with format of ‘.jpg’ from the PASCAL VOV 2012 [29]. Specifically, each watermarked image is conducted via using each watermark of twelve watermarks with fixed transparency, according to Ref. [25]. The number of test watermarked images is 324 and each watermark size is 1.5 times.



Fig. 2. Twelve collected watermarks.

B. Experimental setting

All experiments are conducted on Ubuntu of 20.04 with Intel Xeon Silver 4210 CPU via PyTorch [30] of 1.12 and Python of 3.8. To improve training speed, a GPU of 3090 with CUDA of 10.2 and CuDNN of 8.0.5 is used. Besides, batch size is 8, epoch number is 100 and initial learning rate is $1e-3$, which may get 0.1 of original learning rate in 30th times. More parameters are the same as Ref. [31].

C. Experimental analysis

The proposed SWCNN has three key techniques, i.e., a self-supervised mechanism, a heterogenous architecture of HN and a mixed loss. Their effectiveness and rationality can be analyzed, according to training data, network design principle and image representation, respectively.

A self-supervised mechanism: It is known that existing methods almost depend on paired data (i.e., watermarked images and clean images) in a supervised way to verify robustness of added watermarks in terms of training data [16]. However, corresponding clean images are difficultly obtained in real world. Inspired by Noise2Noise [24], we present a self-supervised mechanism to construct paired watermarked

TABLE I
REMOVING WATERMARK PERFORMANCE OF DIFFERENT METHODS.

Methods	PSNR	SSIM
HN with clean reference images	34.8979	0.9854
HN	31.6688	0.9803
SWCNN	36.9022	0.9893
SWCNN with clean reference images	35.8898	0.9881

images, according to distributions of watermarks. That is, watermarks randomly added in a clean image once is regarded as a clean reference image as well as ground truth. Watermarks randomly added in a clean image another is regarded as a watermarked image as well as input of SWCNN. This can address drawback of no ground truth. Effectiveness of the proposed self-supervised mechanism is verified via both SWCNN and SWCNN with clean reference images in terms of PSNR and SSIM as shown in Table I. To fully verify performance of the proposed self-supervised mechanism, we monitor its performance for different steps of one epoch and different epochs. We can see that the proposed self-supervised mechanism performs better than given paired images, i.e., watermarked image and clean image in Fig.3. According to mentioned illustrations, we can see that the proposed self-supervised mechanism is very effective to remove watermarks.

Heterogenous network: It is known that expressive ability of deep networks is stronger, obtained structural information is more accurate, according to network design principle [32]. For instance, a U-Net combines different components, i.e., convolutional layer, ReLU, max pooling operations, concatenation operations and transpose convolutions to achieve a heterogenous network for extracting more structural information in image denoising [24]. Motivated by that, we also use heterogenous network to mine complementary structural information to verifying quality of given watermarks. We use denoising CNN (DnCNN) [31], fast and flexible denoising CNN (FFDNet) [33], deep Image prior restoration (DIP) [34], WGAN-GP [35], detail-recovery image deraining network (DRD-Net) [36], a deep residual learning algorithm for removing rain streaks (FastDerainNet) [37] and efficient attention fusion network in wavelet domain for demoireing (EAFNWDD) [38] as comparative methods on test dataset for transparency of 0.3 to test performance of the proposed SWCNN. As shown in Table II, effectiveness of heterogenous network is tested via comparing DnCNN, FFDNet, DIP and in terms of PSNR and SSIM for removing watermarks.

Mixed Loss: It is known that image representation, is very important for image restoration. Specifically, structural information from deep network [39] and texture information from perception information [17]. Inspired by that, we use a mixed loss to make a tradeoff between structural and texture information in this paper. That is, a mixed loss is composed of a structural loss and texture loss. The structural loss is conducted via obtained reference image and watermarked image from the proposed self-supervised mechanism in Section II.A. The texture loss is conducted via obtained features of middle

TABLE II
REMOVING WATERMARK PERFORMANCE OF DIFFERENT METHODS FOR TRANSPARENCY OF 0.3.

Methods	PSNR	SSIM
FFDNet [33]	27.8820	0.8778
DIP [34]	29.7473	0.9260
WGAN-GP [35]	31.0752	0.9662
DnCNN [31]	30.1071	0.9620
DRD-Net [36]	28.9090	0.9707
FastDerainNet [37]	32.2593	0.9815
EAFNWDD [38]	33.4744	0.9700
SWCNN (Ours)	36.9022	0.9893

TABLE III
PSNR OF DIFFERENT METHODS FOR DIFFERENT TRANSPARENCY.

Transparency	Methods	PSNR
alpha=0.3	Watermark image	28.9315
	DnCNN [31]	30.1071
	FFDNet [33]	27.8820
	DIP [34]	29.7473
	WGAN-GP [35]	31.0752
	DRD-Net [36]	28.9090
	FastDerainNet [37]	32.2593
	EAFNWDD [38]	33.4744
SWCNN(Ours)	36.9022	
alpha=0.5	Watermark image	24.4613
	DnCNN [31]	29.0817
	FFDNet [33]	26.6991
	DRD-Net [36]	29.5227
	FastDerainNet [37]	29.0564
	EAFNWDD [38]	32.6197
	SWCNN(Ours)	33.6491
	Watermark image	21.5422
alpha=0.7	DnCNN [31]	27.8594
	FFDNet [33]	26.1591
	DRD-Net [36]	31.0825
	FastDerainNet [37]	25.5814
	EAFNWDD [38]	27.0403
	SWCNN(Ours)	30.8870
	Watermark image	18.4946
	alpha=1.0	DnCNN [31]
FFDNet [33]		20.4079
DRD-Net [36]		23.6468
FastDerainNet [37]		20.4333
EAFNWDD [38]		25.9116
SWCNN(Ours)		28.1357

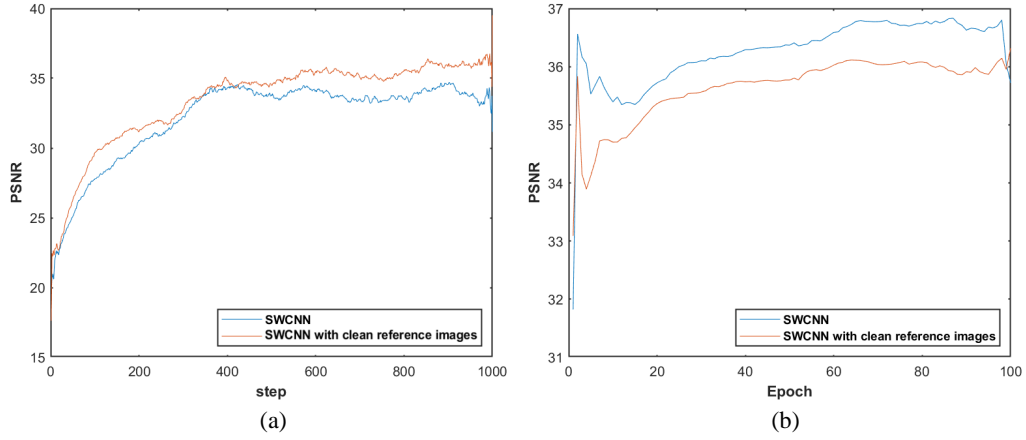


Fig. 3. PSNR of different methods for one epoch and multiple epochs. (a) PSNR of two methods for one epoch , (b) PSNR of two methods for different epochs

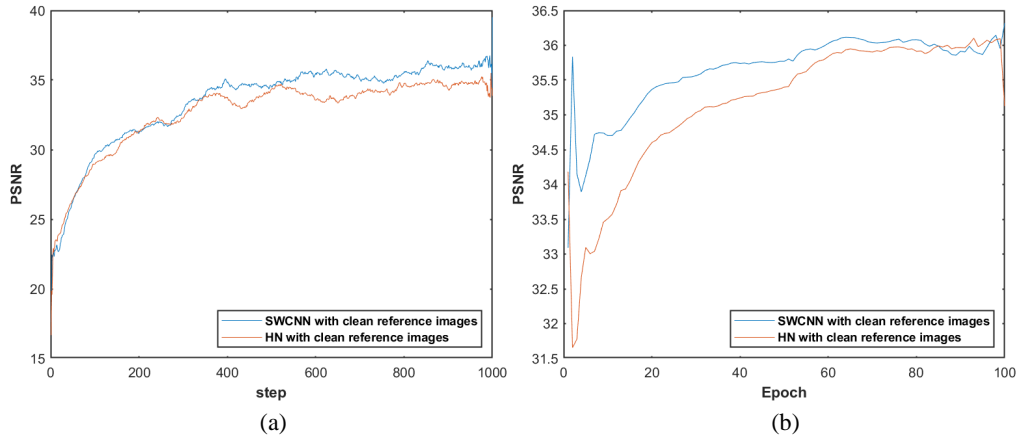


Fig. 4. PSNR of different methods for one epoch and multiple epochs. (a) PSNR of two methods for one epoch, (b) PSNR of two methods for different epochs.

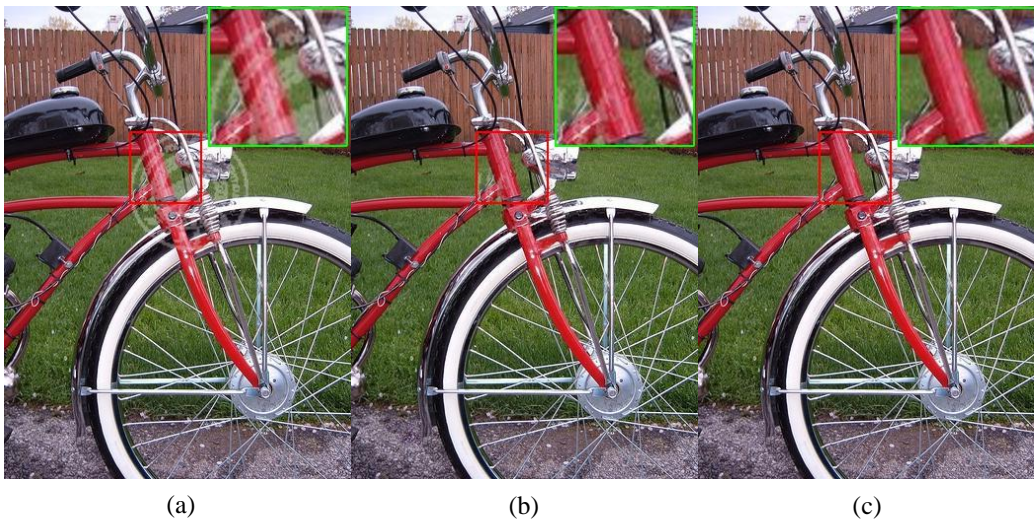


Fig. 5. Visual images of different methods: (a) Watermarked image (29.21dB), (b) HN (32.18dB) and (c) SWCNN (35.75dB).

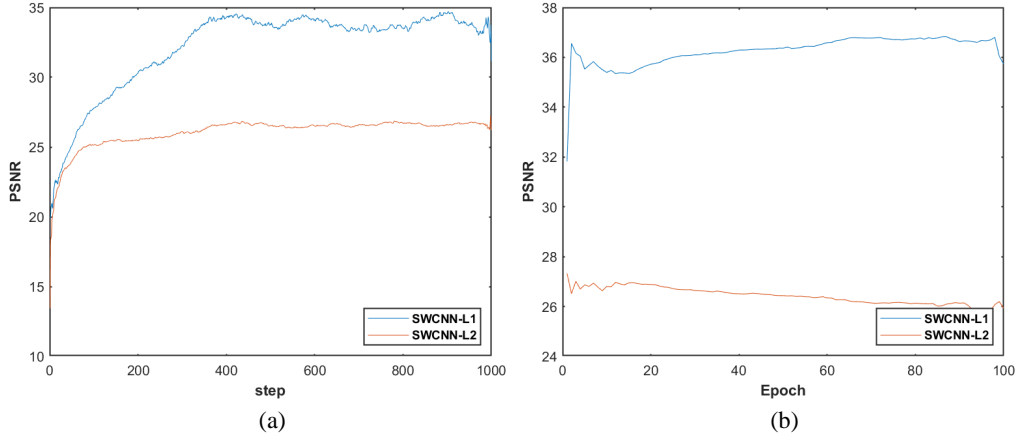


Fig. 6. PSNR of different methods for one epoch and multiple epochs. (a) PSNR of two methods for one epoch, (b) PSNR of two methods for different epochs.

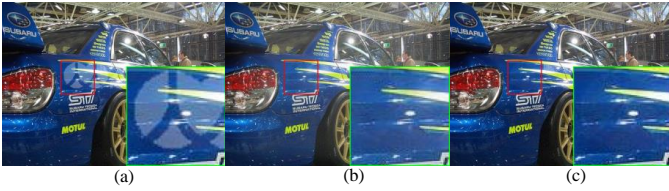


Fig. 7. Visual images of different methods: (a) Watermarked image (29.82dB), (b) SWCNN with L2 (24.90dB), and (c) SWCNN with L1 (37.32dB).

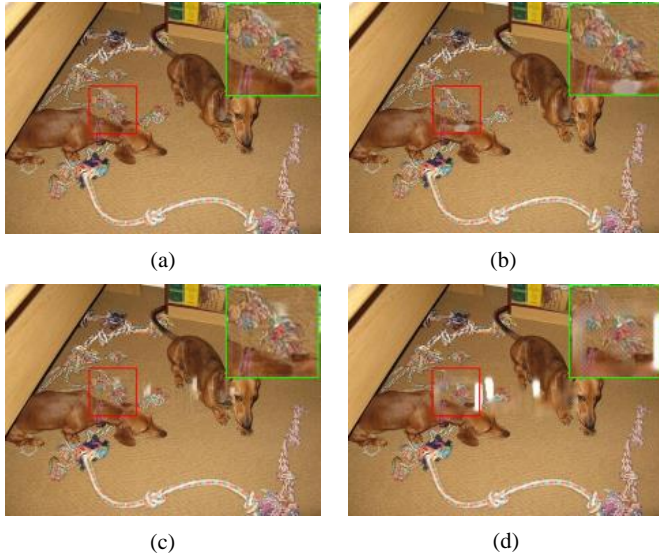


Fig. 8. Visual effects of SWCNN for different transparency in image watermark. (a) SWCNN with transparency of 0.3 (40.72dB), (b) SWCNN with transparency of 0.5 (35.91dB), (c) SWCNN with transparency of 0.7 (33.65dB) and (d) SWCNN with transparency of 1 (26.05dB).

layers of pretrained VGG to act ground truth and predicted image from the HN in Section II.D. The effectiveness of the mixed loss is verified via HN with clean reference images and SWCNN with clean reference images, HN and SWCNN in Table I. That is, a mixed loss above is more effective than a structural loss. To verify robustness of the mixed loss, we

monitor the training process for all the steps of one epoch and all the epochs in terms of PSNR. As shown in Fig.4, we can see that structural loss collaborates texture loss to achieve a mixed loss has better performance than that of a single structural loss for removing watermark. Besides, we enlarge a chosen area of predicted image as an observation area of different methods (i.e., SWCNN and HN) to test performance of mixed loss for image watermark. As illustrated in Fig. 5, we can see that observation area of SWCNN is clear than that of HN, which shows effectiveness of texture loss.

D. Experimental results

We choose several popular image restoration methods, i.e., DnCNN [31], FFDNet [33], DIP [34], WGAN-GP [35], DRD-Net [36], FastDerainNet [37] and EAFNWDD [38] as comparative methods for quantitative and qualitative analysis. Quantitative analysis includes different methods for different transparency and same transparency, complexity (i.e., parameters and flops [40]) and image quality metrics, i.e., natural image quality evaluator (NIQE) [41] and Integrated Local NIQE (ILNIQE) [42] to verify robustness of removing watermarks. For different transparency, we choose different transparency of 0.3, 0.5, 0.7 and 1 to act clean images to conduct experiments. As listed in Table III, we can see that the proposed SWCNN has obtained effective results for different transparency in image watermark. In terms of same transparency, transparency of 0.3 is chosen to conduct experiments. As reported in Table II, we can see that our SWCNN has obtained the highest results in terms of PSNR, which shows effectiveness of SWCNN with certain transparency for image watermark. To evaluate computational cost of SWCNN, we choose complexity to conduct experiments. As described in Table IV, we can see that the proposed method is more competitive than other popular methods, i.e. WGAN-GP and DRD-Net in parameters and flops. To prevent limitations of PSNR and SSIM for low-level vision tasks, image quality evaluators are used to conduct comparative experiments in this paper. Taking into blind image watermark removal ac-

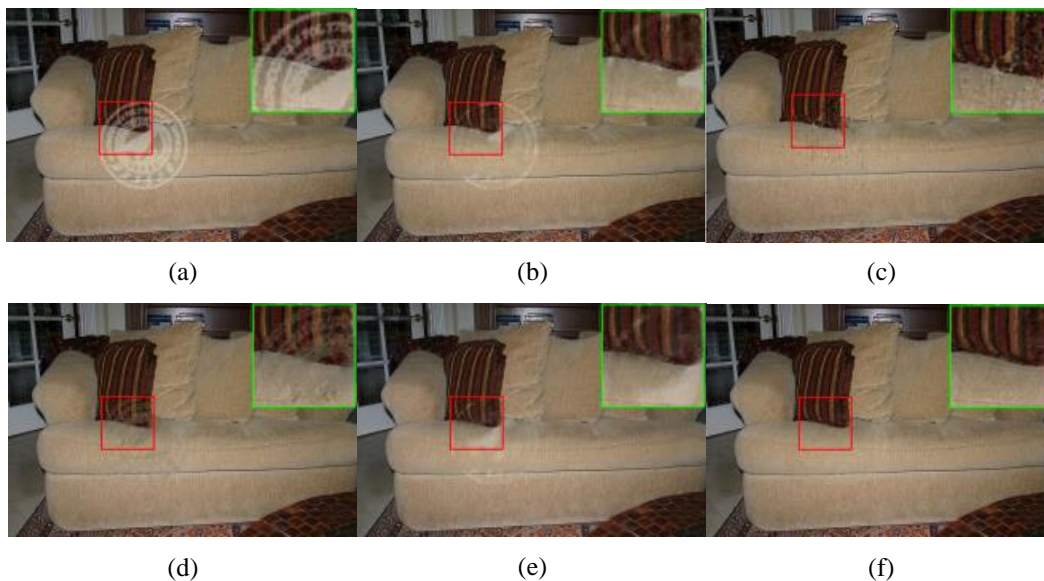


Fig. 9. Visual effects of different methods with transparency of 0.3 for image watermark. (a) Watermarked image (29.82dB), (b) FFDNet (24.95dB), (c) DIP (34.88dB), (d) WGAN-GP (30.59dB), (e) DnCNN (28.26dB) and (f) SWCNN (Ours) (37.32dB).

TABLE IV
COMPLEXITY OF DIFFERENT METHODS ON AN IMAGE WITH 256×256
FOR IMAGE WATERMARK.

Methods	Parameters	Flops
FFDNet [33]	854.688K	14.003G
DIP [34]	2.996M	1.776G
WGAN-GP [35]	3.602M	22.470G
DnCNN [31]	558.336K	36.591G
DRD-Net [36]	2.941M	192.487G
FastDerainNet [37]	336.006K	22.128G
EAFNWDD [38]	52.322M	135.007G
SWCNN (Ours)	700.611K	18.624G

count, popular blind image quality evaluators [43, 44] are prioritized to measure obtained non-watermark images. Li et al. [43] utilized binary patterns of local image structures to extract statistical information to achieve blind image quality assessment. Alternatively, a fusions of statistical information based multiple domains and different channels was presented to address image quality problem [44]. To fairly test quality of obtained images from our SWCNN, we choose blind image quality evaluators with popular codes, i.e., NIQE [41] and (ILNIQE) [42] to test comparative experiments in TABLE VI. As shown in TABLE VI, we can see that obtained SWCNN has obtained the lowest value on both NIQE and ILNIQE than that of other popular methods, i.e., DnCNN, FFDNet and FastDerainNet, which shows it is very competitive for blind image quality assessment. According to mentioned illustrations, the proposed SWCNN is effective in image watermark in terms of quantitative analysis.

To accelerate training speed, L1 rather than L2 is embedded into structural and texture loss. We use quantitative and qualitative analysis to evaluate performance SWCNN with L1 and SWCNN with L2. In terms of quantitative analysis, average

TABLE V
PSNR AND SSIM OF SWCNN WITH DIFFERENT LOSSES.

Methods	PSNR	SSIM
SWCNN-L1	36.9022	0.9893
SWCNN-L2	25.3875	0.9383

TABLE VI
NIQE AND ILNIQE OF DIFFERENT METHODS FOR TRANSPARENCY OF
0.3.

Methods	NIQE [41]	ILNIQE [42]
DnCNN [31]	4.8500	23.2775
FFDNet [33]	5.5887	25.3639
FastDerainNet [37]	4.8070	22.9647
SWCNN(Ours)	4.8039	22.9337

PSNR and SSIM of SWCNN with L1 and SWCNN with L2 on all the test images are used to conduct experiments. As shown in Table V, we can see that SWCNN with L1 is higher PSNR and SSIM than that of SWCNN with L2, which shows effectiveness of loss function with L1 for image watermark. On the other hand, we monitor the training process for all the steps of one epoch and all the epochs in terms of PSNR to verify effectiveness of loss function with L1. As presented in Fig. 6, we can see that SWCNN with L1 has obtained higher values than these of SWCNN with L2 for all the steps of one epoch and multiple epochs, which shows effectiveness of loss function with L1 for the whole training process in image watermark. In terms of qualitative analysis, we can see that observation area of SWCNN with L1 is clear than that of SWCNN with L2, which shows effectiveness of loss function with L1 as shown in Fig. 7. According to quantitative and qualitative analysis, loss function with L1 is suitable to SWCNN for image watermark removal.

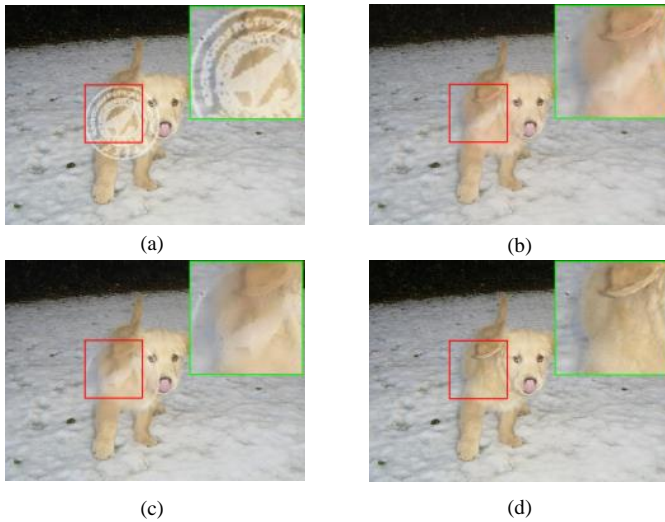


Fig. 10. Visual effects of different methods with transparency of 0.5 for image watermark. (a) Watermarked image (34.24dB), (b) DnCNN (33.46dB), (c) FFDNet (31.50dB) and (d) SWCNN (Ours) (40.89dB).

Qualitative analysis: we amplify an area of different methods as observation area to evaluate visual effects via their clarity. Fig. 8 shows observation areas of our SWCNN for different transparency, which shows our method is robust for different transparency. Fig. 9 and Fig. 10 show that the proposed SWCNN is clearer than other popular methods, i.e., FFDNet and DnCNN for removing watermarks. That shows the proposed SWCNN is effective for image watermark removal in terms of qualitative analysis. According to quantitative analysis and qualitative analysis, we can see that the proposed SWCNN is suitable to image watermark removal.

IV. CONCLUSION

In this paper, we propose a self-supervised convolutional neural network for image watermark removal as well as SWCNN. Proposed SWCNN uses a self-supervised way to construct reference images rather than given paired training samples, according to watermark distribution. A heterogeneous U-Net and a mixed loss are used to make a tradeoff between structural and texture information. Besides, a watermark dataset with twelve different watermarks for different coverages is conducted to verify robustness of the proposed watermark method. Our SWCNN is competitive compared with popular CNNs in terms of different transparency, visual effects, complexities for image watermark removal. Evaluations on widely used benchmarks demonstrate the effectiveness of our proposed method.

REFERENCES

- [1] G. W. Braudaway, "Protecting publicly-available images with an invisible image watermark," in *Proceedings of international conference on image processing*, vol. 1. IEEE, 1997, pp. 524–527.
- [2] X.-L. Liu, C.-C. Lin, and S.-M. Yuan, "Blind dual watermarking for color images' authentication and copyright protection," *IEEE Transactions on Circuits and Systems for Video Technology*, vol. 28, no. 5, pp. 1047–1055, 2016.
- [3] S.-J. Lee and S.-H. Jung, "A survey of watermarking techniques applied to multimedia," in *ISIE 2001. 2001 IEEE International Symposium on Industrial Electronics Proceedings (Cat. No. 01TH8570)*, vol. 1. IEEE, 2001, pp. 272–277.
- [4] H.-H. Tsai and D.-W. Sun, "Color image watermark extraction based on support vector machines," *Information Sciences*, vol. 177, no. 2, pp. 550–569, 2007.
- [5] P. H. Wong, O. C. Au, and Y. M. Yeung, "Novel blind multiple watermarking technique for images," *IEEE transactions on circuits and systems for video technology*, vol. 13, no. 8, pp. 813–830, 2003.
- [6] Y. Hu, S. Kwong, and J. Huang, "An algorithm for removable visible watermarking," *IEEE Transactions on Circuits and Systems for Video Technology*, vol. 16, no. 1, pp. 129–133, 2005.
- [7] Y. Hu and B. Jeon, "Reversible visible watermarking and lossless recovery of original images," *IEEE Transactions on Circuits and Systems for Video Technology*, vol. 16, no. 11, pp. 1423–1429, 2006.
- [8] J. Park, Y.-W. Tai, and I. S. Kweon, "Identigram/watermark removal using cross-channel correlation," in *2012 IEEE Conference on Computer Vision and Pattern Recognition*. IEEE, 2012, pp. 446–453.
- [9] A. Westfeld, "A regression-based restoration technique for automated watermark removal," in *Proceedings of the 10th ACM workshop on Multimedia and security*, 2008, pp. 215–220.
- [10] H. Santoyo-Garcia, E. Frago-Navarro, R. Reyes-Reyes, G. Sanchez-Perez, M. Nakano-Miyatake, and H. Perez-Meana, "An automatic visible watermark detection method using total variation," in *2017 5th International Workshop on Biometrics and Forensics (IWBF)*. IEEE, 2017, pp. 1–5.
- [11] R. Cong, N. Yang, C. Li, H. Fu, Y. Zhao, Q. Huang, and S. Kwong, "Global-and-local collaborative learning for co-salient object detection," *arXiv preprint arXiv:2204.08917*, 2022.
- [12] R. Cong, Y. Zhang, L. Fang, J. Li, Y. Zhao, and S. Kwong, "Rnet: Relational reasoning network with parallel multiscale attention for salient object detection in optical remote sensing images," *IEEE Transactions on Geoscience and Remote Sensing*, vol. 60, pp. 1–11, 2021.
- [13] C. Tian, Y. Xu, W. Zuo, C.-W. Lin, and D. Zhang, "Asymmetric cnn for image superresolution," *IEEE Transactions on Systems, Man, and Cybernetics: Systems*, 2021.
- [14] X. Chen, W. Wang, Y. Ding, C. Bender, R. Jia, B. Li, and D. Song, "Leveraging unlabeled data for watermark removal of deep neural networks," in *ICML workshop on Security and Privacy of Machine Learning*, 2019, pp. 1–6.
- [15] J. Wang, H. Wu, X. Zhang, and Y. Yao, "Watermarking in deep neural networks via error back-propagation," *Electronic Imaging*, vol. 2020, no. 4, pp. 22–1, 2020.
- [16] D. Cheng, X. Li, W.-H. Li, C. Lu, F. Li, H. Zhao, and W.-S. Zheng, "Large-scale visible watermark detection and removal with deep convolutional networks," in *Chinese Conference on Pattern Recognition and Computer Vision (PRCV)*. Springer, 2018, pp. 27–40.
- [17] X. Li, C. Lu, D. Cheng, W.-H. Li, M. Cao, B. Liu, J. Ma, and W.-S. Zheng, "Towards photo-realistic visible watermark removal with conditional generative adversarial networks," in *International Conference on Image and Graphics*. Springer, 2019, pp. 345–356.
- [18] Z. Cao, S. Niu, J. Zhang, and X. Wang, "Generative adversarial networks model for visible watermark removal," *IET Image Processing*, vol. 13, no. 10, pp. 1783–1789, 2019.
- [19] X. Chen, W. Wang, C. Bender, Y. Ding, R. Jia, B. Li, and D. Song, "Re-fit: a unified watermark removal framework for deep learning systems with limited data," in *Proceedings of the 2021 ACM Asia Conference on Computer and Communications Security*, 2021, pp. 321–335.
- [20] X. Cun and C.-M. Pun, "Split then refine: stacked attention-guided resunets for blind single image visible watermark removal," in *Proceedings of the AAAI Conference on Artificial Intelligence*, vol. 35, no. 2, 2021, pp. 1184–1192.

- [21] Y. Liu, Z. Zhu, and X. Bai, "Wdnet: Watermark-decomposition network for visible watermark removal," in *Proceedings of the IEEE/CVF Winter Conference on Applications of Computer Vision*, 2021, pp. 3685–3693.
- [22] L. Fu, B. Shi, L. Sun, J. Zeng, D. Chen, H. Zhao, and C. Tian, "An improved u-net for watermark removal," *Electronics*, vol. 11, no. 22, p. 3760, 2022.
- [23] C. Song, S. Sudirman, M. Merabti, and D. Llewellyn-Jones, "Analysis of digital image watermark attacks," in *2010 7th IEEE Consumer Communications and Networking Conference*. IEEE, 2010, pp. 1–5.
- [24] J. Lehtinen, J. Munkberg, J. Hasselgren, S. Laine, T. Karras, M. Aittala, and T. Aila, "Noise2noise: Learning image restoration without clean data," *arXiv preprint arXiv:1803.04189*, 2018.
- [25] T. Dekel, M. Rubinstein, C. Liu, and W. T. Freeman, "On the effectiveness of visible watermarks," in *Proceedings of the IEEE Conference on Computer Vision and Pattern Recognition*, 2017, pp. 2146–2154.
- [26] A. Krizhevsky, I. Sutskever, and G. E. Hinton, "Imagenet classification with deep convolutional neural networks," *Advances in neural information processing systems*, vol. 25, 2012.
- [27] A. L. Maas, A. Y. Hannun, A. Y. Ng *et al.*, "Rectifier nonlinearities improve neural network acoustic models," in *Proc. icml*, vol. 30, no. 1. Atlanta, Georgia, USA, 2013, p. 3.
- [28] D. P. Kingma and J. Ba, "Adam: A method for stochastic optimization," *arXiv preprint arXiv:1412.6980*, 2014.
- [29] M. Everingham, S. Eslami, L. Van Gool, C. K. Williams, J. Winn, and A. Zisserman, "The pascal visual object classes challenge: A retrospective," *International journal of computer vision*, vol. 111, no. 1, pp. 98–136, 2015.
- [30] A. Paszke, S. Gross, S. Chintala, G. Chanan, E. Yang, Z. DeVito, Z. Lin, A. Desmaison, L. Antiga, and A. Lerer, "Automatic differentiation in pytorch," 2017.
- [31] K. Zhang, W. Zuo, Y. Chen, D. Meng, and L. Zhang, "Beyond a gaussian denoiser: Residual learning of deep cnn for image denoising," *IEEE transactions on image processing*, vol. 26, no. 7, pp. 3142–3155, 2017.
- [32] Y. Tai, J. Yang, X. Liu, and C. Xu, "Memnet: A persistent memory network for image restoration," in *Proceedings of the IEEE international conference on computer vision*, 2017, pp. 4539–4547.
- [33] K. Zhang, W. Zuo, and L. Zhang, "Ffdnet: Toward a fast and flexible solution for cnn-based image denoising," *IEEE Transactions on Image Processing*, vol. 27, no. 9, pp. 4608–4622, 2018.
- [34] D. Ulyanov, A. Vedaldi, and V. Lempitsky, "Deep image prior," in *Proceedings of the IEEE conference on computer vision and pattern recognition*, 2018, pp. 9446–9454.
- [35] J. Yu, Z. Lin, J. Yang, X. Shen, X. Lu, and T. S. Huang, "Generative image inpainting with contextual attention," in *Proceedings of the IEEE conference on computer vision and pattern recognition*, 2018, pp. 5505–5514.
- [36] S. Deng, M. Wei, J. Wang, L. Liang, H. Xie, and M. Wang, "Drd-net: Detail-recovery image deraining via context aggregation networks," *arXiv preprint arXiv:1908.10267*, 2019.
- [37] X. Wang, Z. Li, H. Shan, Z. Tian, Y. Ren, and W. Zhou, "Fastderainnet: A deep learning algorithm for single image deraining," *IEEE Access*, vol. 8, pp. 127 622–127 630, 2020.
- [38] C. Sun, H. Lai, L. Wang, and Z. Jia, "Efficient attention fusion network in wavelet domain for demoireing," *IEEE Access*, vol. 9, pp. 53 392–53 400, 2021.
- [39] P. Sahu, D. Yu, M. Dasari, F. Hou, and H. Qin, "A lightweight multi-section cnn for lung nodule classification and malignancy estimation," *IEEE journal of biomedical and health informatics*, vol. 23, no. 3, pp. 960–968, 2018.
- [40] R. Dolbeau, "Theoretical peak flops per instruction set: a tutorial," *The Journal of Supercomputing*, vol. 74, no. 3, pp. 1341–1377, 2018.
- [41] A. Mittal, R. Soundararajan, and A. C. Bovik, "Making a "completely blind" image quality analyzer," *IEEE Signal processing letters*, vol. 20, no. 3, pp. 209–212, 2012.
- [42] L. Zhang, L. Zhang, and A. C. Bovik, "A feature-enriched completely blind image quality evaluator," *IEEE Transactions on Image Processing*, vol. 24, no. 8, pp. 2579–2591, 2015.
- [43] Q. Wu, Z. Wang, and H. Li, "A highly efficient method for blind image quality assessment," in *2015 IEEE International Conference on Image Processing (ICIP)*. IEEE, 2015, pp. 339–343.
- [44] Q. Wu, H. Li, F. Meng, K. N. Ngan, B. Luo, C. Huang, and B. Zeng, "Blind image quality assessment based on multichannel feature fusion and label transfer," *IEEE Transactions on Circuits and Systems for Video Technology*, vol. 26, no. 3, pp. 425–440, 2015.